

# Label-free optical imaging of membrane potential

Hyeon Jeong Lee<sup>1,2,4,a</sup>, Ying Jiang<sup>4,5,a</sup> and Ji-Xin Cheng<sup>2,3,4</sup>

## Abstract

Offering high temporal resolution, voltage imaging is an important and essential technique in neuroscience. Among different optical imaging approaches, the label-free approach remains attractive because exogenous chromophores are not used in this approach. The intrinsic voltage-indicating signals arising from membrane deformation, membrane spectral change, phase shift, light scattering, and membrane hydration have been reported. First demonstrated 70 years ago, label-free optical imaging of membrane potential is still at an early stage, and the field is challenged by the relatively small signals generated by the intrinsic optical properties. We review major contrast mechanisms used for label-free voltage imaging and discuss several recent exciting advances that could potentially enable membrane potential imaging in mammalian neurons at high speed and high sensitivity.

## Addresses

<sup>1</sup> College of Biomedical Engineering and Instrument Science, Zhejiang University, Hangzhou, Zhejiang 310027, China

<sup>2</sup> Department of Electrical and Computer Engineering, Boston University, Boston, MA 02215, USA

<sup>3</sup> Department of Biomedical Engineering, Boston University, Boston, MA 02215, USA

<sup>4</sup> Photonics Center, Boston University, Boston, MA 02215, USA

<sup>5</sup> Graduate Program for Neuroscience, Boston University, Boston, MA 02215, USA

Corresponding author: Cheng, Ji-Xin ([jxcheng@bu.edu](mailto:jxcheng@bu.edu))

<sup>a</sup> These authors contributed equally.

Current Opinion in Biomedical Engineering 2019, 12:118–125

This review comes from a themed issue on **Neural Engineering: High Resolution Cell Imaging**

Edited by **John A White** and **Xue Han**

<https://doi.org/10.1016/j.cobme.2019.11.001>

2468-4511/© 2019 Elsevier Inc. All rights reserved.

## Keywords

Label-free, Voltage imaging, Birefringence, Phase imaging, Second harmonic generation, Stimulated Raman scattering.

## Abbreviations

OCT, optical coherence tomography; XPS, cross polarized signal; SHG, second harmonic generation; CARS, coherent anti-Stokes Raman scattering; SRS, stimulated Raman scattering; MIP, mid-infrared photothermal microscopy; SFG, sum frequency generation; THG, third harmonic generation; AP, action potential.

## Introduction

Membrane potential is critical for many physiological processes. The membrane voltage is a form of signaling for cellular communications, especially for excitable

cells. The standard approach for monitoring membrane potential is by patch clamp electrophysiology. The direct measurement of electrical signals provides extremely high sensitivity and temporal resolution, making it the gold standard in neuroscience. However, patch clamp is an invasive method performed at single position or occasionally at a few positions. The need for performing multisite measurement becomes more apparent as an increasing number of research suggests that the neural network forms a functional unit of the nervous system [1]. The neural network functioning can be better studied using optical recording approaches, with its advantages of noninvasiveness and capability of mapping the membrane potentials in a neural circuit at subcellular to multicellular levels [2–4]. Although it is challenging to optically detect membrane voltage, the significant advances in technological innovation and development of new contrast mechanisms have made optical voltage recording an important field in neuroscience.

The first observation of changes in intrinsic optical property during neuron activation was reported nearly 70 years ago [5]. Since then, various contrast mechanisms have been studied and demonstrated in nonmammalian neurons or nerve bundles [6–11]. However, limited by the weak intrinsic signal, optical measurement in mammalian neurons, which are even smaller and more transparent than invertebrate neurons, remains extremely challenging. Voltage-sensitive dyes with strong signals and fast-response kinetics were developed, offering the capability for large-scale monitoring of neural activities [12–14]. These reporters have been a powerful tool for imaging neural activities in mammalian neurons and tissues. More recently, genetically encoded voltage indicators were developed, providing advantages of targeting specific cell populations and low-invasive staining of neurons [15]. These advantages of genetic targeting allow monitoring neural activities of specific cell types in brain tissues and *in vivo* preparation [4,16,17]. With the improved sensitivity and signal to noise ratio, fast spiking activities and sub-threshold electrical events were detected both *in vivo* and in live animals using these voltage imaging techniques [18–21].

On the other hand, label-free optical recording remains attractive because of its own merits [22]. First, label-free imaging requires minimal sample preparation. Second, there is no concern for cytotoxicity or perturbation of membrane properties caused by labeling. Third, label-free imaging is free of photobleaching

Table 1

## Label-free optical imaging of membrane potential.

Imaging modality	Contrast mechanism	Biological systems	Sensitivity	Imaging speed	Reference
Transmission	Membrane deformation	Mammalian neurons	Single AP with averaging	1603 Hz frame rate	[33]
OCT	Scattering	Aplysia neurons	Single AP with averaging	1 KHz line rate	[36]
Interferometric imaging	Phase changes	HEK293 cells	Single AP with averaging	1 KHz frame rate	[39]
SHG	Membrane hydration	Mammalian neurons	Membrane depolarization	1.7 Hz frame rate	[47]
SRS	Chemical bond vibration	Mammalian neurons, brain slices	Single AP, membrane depolarization	10 Hz frame rate, 750 Hz line rate	[61]

OCT, optical coherence tomography; SHG, second harmonic generation; SRS, stimulated Raman scattering microscopy; AP, action potential.

complications, allowing long-term measurement. Forth, label-free imaging is of interest for clinical measurement and translation to human subjects. These factors have driven continuous attempts for improving the detection sensitivity of intrinsic optical signals and developing new intrinsic contrasts for membrane potentials.

Here, we review recent advances, mainly over the past 5 years, in label-free imaging techniques developed for recording membrane potential toward single-cell resolution. These technologies are summarized in Table 1, sorted by the contrast mechanisms. We note that label-free, indirect imaging of neural activity through measurement of blood flow, and oxygenation has been demonstrated (for reviews, refer to the study by Boas and Dunn [23] and Morone [24]). Those techniques are beyond the scope of this review, as they are unlikely to provide membrane voltage dynamics with single-cell precision.

## Label-free voltage imaging by linear optics

### Change in mechanical properties of membrane

Although neural activities are studied mainly by electrophysiology, this process is more than just an electric wave. It involves dynamics of all the structures: extracellular fluid, the biomembrane, ion channel proteins, and the axoplasm. A large number of studies have shown transient mechanical changes accompanying action potentials [7,8,25–33]. In fact, such intrinsic changes of cell morphology are among the earliest properties exploited to visualize action potentials in invertebrate nervous systems apart from electrophysiology. Cohen and Keynes. [6,7] first reported the changes of neuronal structures, including axon diameter and retardation, during action potential propagation in the squid giant axons. The observation is later confirmed by others [8,25,26,28]. Owing to the development in atomic force microscopy with subnanometer detection sensitivity, Gonzalez-Perez *et al.* [31] measured mechanical changes during action potential propagation. Membrane displacement in the order of 0.3–1.2 nm was observed in a single axon from lobster, which is proportional to the changes in voltage. Although these studies were mostly carried out in invertebrate nerves, in which the

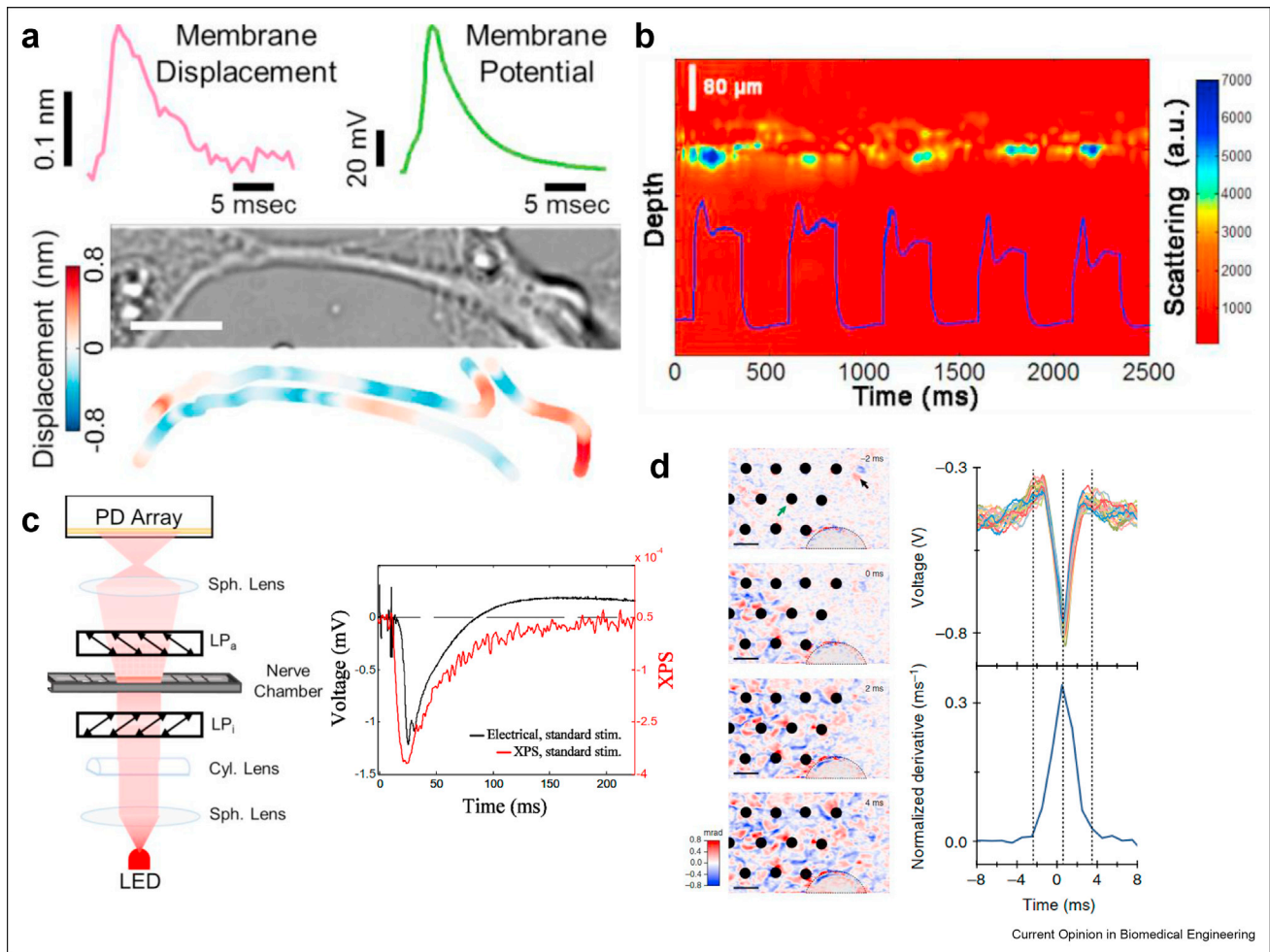
morphological changes are prominent because of large axon diameters, they gave rise to the theory that a mechanical wave accompanies action potential propagation in axons. A series of studies focused on modeling of this mechanical coupling [30,32,34] and predicted the similar membrane displacement on rat hippocampal neurons [30]. Later, Yang *et al.* [33] further validated these biophysical models in mammalian neurons by imaging rat hippocampal neurons using a simple optical microscope with a high-speed camera (Figure 1a). Membrane displacements were identified by an edge-tracking approach, indicating an average membrane displacement of 0.3 nm during action potential. Importantly, the multiplex capability of the imaging system enabled visualization of action potential initiation and propagation from soma to distal axons (Figure 1a), providing spatial information of the morphological changes [33].

### Change in optical properties of membrane

Apart from the morphological changes, pressure and thermal events during action potential also change the intrinsic optical properties of the neurons or tissue. Indirect optical detection of refractive index or birefringence changes offers a higher sensitivity than the direct measurement of the nanoscale membrane displacement.

The first optical recording of neural activity reported was using scattered light. In 1949, Hill and Keynes [5] observed the change in light scattering from crab leg nerves when activated with a train of stimuli. This phenomenon was reproduced by multiple studies in different biological systems, in which signal is improved over averaging to detect a single action potential [6,9,11,35]. In 1991, Stepnoski *et al.* [11] optically resolved action potentials in a single Aplysia neuron using a dark field illumination scheme. It was proposed that the detected scattered light arises from changes in alignment of dipoles in the membrane. Almost two decades later, Graf *et al.* [36] established the correlation between light scattering intensity and membrane voltage in Aplysia neurons by optical coherence tomography (OCT) and optical coherence microscopy

Figure 1



**Label-free linear optical imaging of membrane voltage.** (a) Quantification of membrane displacement and corresponding action potential trace of rat hippocampal neurons by transmission imaging, and mapping of local membrane displacement at the peak of an action potential. Reprinted with permission from Yang et al. [33]. (b) M-mode scattering OCT image and membrane voltage of a single Aplysia bag cell neuron in culture during a train of stimulation pulses. Reprinted with permission from Graf et al. [36]. (c) Schematic of experimental setup for detecting XPS based on birefringence changes during an action potential. Recorded XPS signal and the corresponding electrical signal in lobster nerve are compared on the right. Reprinted with permission from Badreddine et al. [37]. (d) Left: Propagation of the action potential across the field of view over 6 ms acquired by full-field interferometric imaging of HEK293 cells. Right: Comparison between the electrical signal on the reference electrode and the time derivative of the optical signal. Reprinted with permission from Ling et al. [39]. XPS, cross polarized signals; OCT, optical coherence tomography.

(Figure 1b). Birefringence is another important optical property of neural tissues. Because neurons and nerves are structurally anisotropic, they inherently exhibit a static birefringence contributed by the cytoskeleton, membrane phospholipids, proteins, and surrounding environment such as the myelin sheath. The birefringence change accompanied by action potential was first observed on crab axons and squid giant axons [35]. Badreddine et al. [37] recorded the propagation of action potential along the lobster nerve by measuring the cross polarized signals (XPS) (Figure 1c). However, scattering- and birefringence-based methods have not been applied to mammalian neurons with single neuron resolution, likely because of the fact that mammalian

neurons have significantly smaller size (10 μm) compared with that of Aplysia (200–500 μm), which makes the detection difficult.

#### Change in phase shift

Phase-sensitive interferometry is one of the most sensitive methods to detect nanoscale changes in optical path length and has been used to probe the small changes of light path during action potential [38,39]. Interferometry is achieved by the superposition of a reference beam and a signal beam, where the signal beam carries the object information of interest. In different apparatus, the reference beam could be provided by a spatially filtered plane wave or a spatially

offset beam at the sample plane. The action potential-induced phase change is extracted through polarization change or interference fringe change [38,39]. Laporta and Kleinfeld [38] demonstrated an interferometric measurement of action potential in lobster nerve with single point detection. Batabyal *et al.* [40] recorded a network of neural activity in cultured mammalian neurons sandwiched between two cover glasses, potentially resolving single action potentials. More recently, Ling *et al.* [39] demonstrated full-field interferometric imaging of HEK293 cells on a multielectrode array setup. The phase-shift signal correlates with the electrophysiology signal, and a 3 nm change in optical path was reported (Figure 1d). However, extensive averaging was required to achieve reasonable signal to noise ratio.

### Label-free voltage imaging by nonlinear optical microscopy

The intrinsic optical properties discussed above usually adopts linear optical techniques that allow high speed, wide-field imaging, but its signal is deteriorated heavily in highly scattering samples such as brain tissues. Furthermore, lack of longitudinal sectioning capability limits the application in deep-tissue voltage imaging. The advantages that are inherent to nonlinear optical techniques, including axial sectioning and penetration into thick tissue samples, offer opportunities to address these challenges in label-free voltage imaging. We note the innovation reported by Fischer *et al.*, in 2008, in which the linear process of light scattering changes is probed using a nonlinear optical technique known as self-phase modulation, to detect population electrical activity in brain slices [41]. Here, we focus on a few new contrast mechanisms discovered and developed recently for nonlinear optical imaging of single membrane potential.

#### Change in membrane hydration

The signal from second harmonic generation (SHG) arises from noncentrosymmetric or anisotropic materials and is inherently sensitive to interfacial processes, chemical changes, and electrochemical responses [42]. Therefore, SHG is one of the important techniques to study noncentral symmetric structures. In the voltage imaging application, various voltage-sensitive molecules with asymmetric structure were developed for SHG voltage imaging in mammalian neurons [43] and brain slices [44–46]. Only recently, label-free SHG imaging of membrane potential in mammalian neurons has been achieved [47] (Figure 2a and b). Technological innovation in this study involves structurally illuminated wide-field imaging scheme that enhances the imaging throughput of SHG microscopy by three orders of magnitude [42,48]. Such improvement allows detection of weak SHG processes such as orientational ordering of interfacial water. Water molecule orientation is highly dynamic and sensitive to the

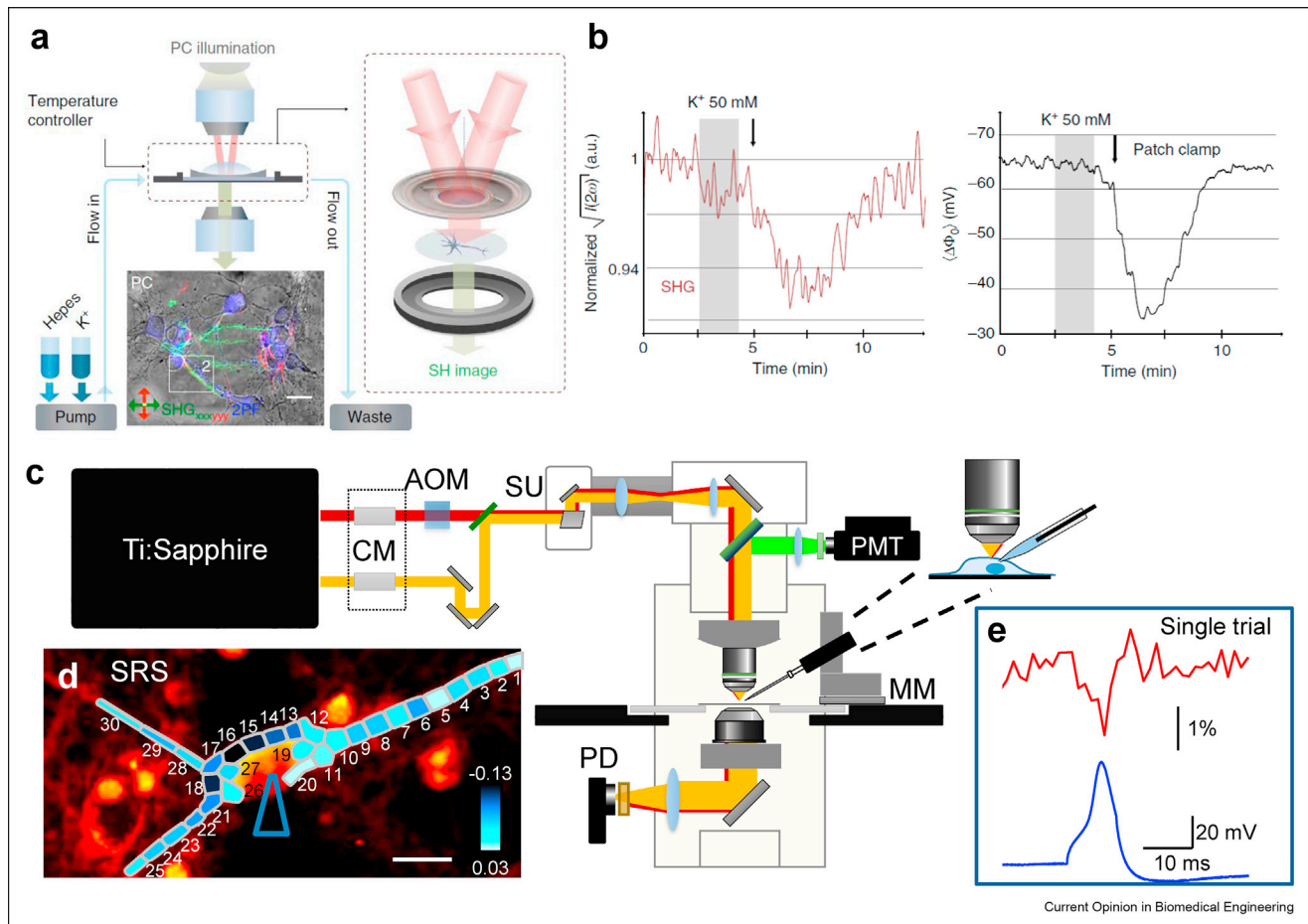
surface charges [49,50]. Using the high-throughput wide-field SHG microscope, membrane structure and dynamics were plotted on millisecond time scales by imaging water aligned by charge–dipole interactions between water molecules and charged lipids [51]. Later, the membrane water orientation is used to optically record membrane potential in mammalian neurons [47]. The SHG intensity decreased upon the application of high  $K^+$  extracellular buffer, which agrees well with the electrophysiology measurements (Figure 2b). Furthermore, the spatiotemporal dynamics of membrane potential and  $K^+$  ion efflux were mapped in cultured neurons within 600 ms intervals [47]. Although the imaging speed in the hundreds of millisecond range is not fast enough for capturing action potentials and firings, the significant improvement in the optical system and the importance of water/lipid interactions promise possibilities of wide-field SHG imaging for mapping membrane potentials in real time.

#### Change in membrane vibrational spectral profile

Vibrational spectroscopy provides qualitative and quantitative information on the chemical and physical properties of molecules. Specifically, chemical bonds in a molecule vibrate in many ways, generating different vibrational modes. The vibrational energy can be measured by spectroscopic techniques. Among them, Raman spectroscopy uses scattered light to obtain knowledge about molecular information, including molecular structure, orientation, bonding, and symmetry. In addition to the characterization of molecular properties, the Raman spectral change of molecules induced by microenvironment such as pH [52], electrochemical environment [53], and solvent shell of ions [54] can be measured for functional analysis. However, Raman spectroscopic characterization of membrane potential in living cells was not possible because spontaneous Raman scattering is naturally a very weak process.

The recently developed coherent Raman scattering microscopy [55], including coherent anti-Stokes Raman scattering (CARS) and stimulated Raman scattering (SRS), overcomes such barrier. CARS and SRS have shown promise in biomedical imaging applications with an acquisition speed of 3–5 orders of magnitude faster than spontaneous Raman microscopes [56,57]. Especially, CARS or SRS microscopy has been successfully applied to study membrane structures, such as membrane lipid ordering [58] and phase separation [59]. Furthermore, SRS microscopy has been applied to show correlation of membrane spectral profile with transmembrane potential in model membrane [60]. These studies indicate the capability of coherent Raman imaging technique for probing membrane action potential which happens in the millisecond time scale.

Figure 2



**Label-free nonlinear optical imaging of membrane voltage.** (a) Schematic of SHG imaging setup in a wide-field double beam transmission geometry for imaging cultured cortical neurons. The extracellular buffer is controlled by a constant flow of solution via a peristaltic perfusion system. Scale bar: 20 μm. (b) The square-rooted spatially averaged SHG signal plotted over time (left) and compared with the whole-cell current clamp recording shown on the right. The arrow indicates the time neurons encountered the high K<sup>+</sup> buffer. (a–b) are reprinted with permission from Didier et al. [47]. (c) Schematic of hyperspectral SRS imaging setup synchronized with patch clamp electrophysiology. (d) SRS image (2930 cm<sup>-1</sup>) of a cortical neuron under somatic voltage-clamp control. Color map of SRS intensity changes in the 30 regions of interest upon depolarization is superimposed scale bar: 10 μm. (e) Single-trial SRS time trace (red) of the neuron with a simultaneous current clamp recording (blue). (c–e) are reprinted with permission from Lee et al. [61]. Copyright 2017 American Chemical Society. CM, chiral media; AOM, acousto-optic modulator; SU, scanning unit; PMT, photomultiplier tube; MM, micromanipulator; PD, photodiode; SHG, second harmonic generation; SRS, stimulated Raman scattering.

By synchronizing the voltage-clamp recording with a frame-by-frame hyperspectral SRS imaging scheme, Lee and Zhang et al. [61] identified spectroscopic signature of neuronal membrane potentials (Figure 2c–e). The SRS spectral profile analysis of neuronal membrane under somatic voltage-clamp control revealed that CH<sub>3</sub> vibration at 2930 cm<sup>-1</sup>, mainly contributed by proteins, is sensitive to membrane voltage. The origin of the spectroscopic change is attributed to ion interactions on the CH<sub>3</sub> Fermi resonance peak, which is partially dependent on Na<sup>+</sup> ion influx [61]. The SRS voltage imaging allowed mapping of membrane potential with subcellular resolution (Figure 2d), and high-speed imaging for multineuron analysis in mouse brain slices.

Importantly, by adopting a dual-SRS balanced detection scheme to further enhance signal-to-noise ratio, label-free single-trial action potential imaging was demonstrated in a single mammalian neuron [61] (Figure 2e). As SRS imaging relies on pixel-by-pixel scanning, a line-scanning mode was applied to capture single action potentials of several milliseconds in this study. With continuous efforts to improve the imaging and spectral acquisition speed, SRS imaging holds great potential as a novel label-free voltage imaging technique.

### Discussion and outlook

Label-free voltage imaging has been sought because of its advantages that are discussed previously. Despite the

efforts over many years, the label-free imaging modalities are still at the early state for applying to high-speed voltage imaging. Overall, intrinsically weak signal, low sensitivity, and slow imaging speed are some of the common challenges in these techniques. To date, none of the current label-free methods have achieved voltage imaging in live animals. The mammalian brain is a complex and highly scattering medium containing neurons, glial cells, extracellular matrix, and lipid-rich structures. These properties are not ideal for label-free voltage imaging methods that use light scattering, birefringence, or phase detection. Nonlinear optics-based methods have demonstrated its capability of imaging more complicated systems such as brain slices [61–63] and even mouse brain *in vivo* [64]. However, advances in imaging speed are required for resolving single action potentials with large area coverage.

Besides the existing strategies, new imaging modalities and contrast mechanisms are expected to be developed. Sum frequency generation (SFG) and third harmonic generation (THG) are two other nonlinear optical processes for label-free imaging of biological tissues [65–67]. Both SFG and THG microscopy has been demonstrated to provide excellent contrast for axon fibers and extracellular matrix [65,67]. However, the voltage-sensitive signatures are yet to be identified. Another promising label-free imaging modality is based on infrared spectrum. Jiang *et al.* [68]. identified the infrared spectrum changes in sensory rhodopsin II, a membrane photoreceptor protein of Archaea, in response to voltage changes in the substrate. The recently developed mid-infrared photothermal microscopy offers new opportunities by applying infrared spectroscopy to map live biological samples [69–71], which is beyond the reach of conventional infrared imaging capabilities. The pixel dwell time of the aforementioned work is down to 500  $\mu$ s, which will be suitable for resolving action potentials. In addition, new advances such as wide-field detection have been demonstrated recently to further improve imaging speed [72]. We anticipate that infrared-based imaging is a promising technique for voltage imaging. Overall, continuous efforts are expected to improve current label-free imaging modalities and develop new intrinsic contrast mechanism for probing membrane potential.

## Conflict of interest statement

Nothing declared.

## Acknowledgements

This work is supported by R01NS109794 to JXC.

## References

Papers of particular interest, published within the period of review, have been highlighted as:

- of special interest
  - of outstanding interest
1. Yuste R: **From the neuron doctrine to neural networks.** *Nat Rev Neurosci* 2015, **16**:487.
  2. Wilt BA, *et al.*: **Advances in light microscopy for neuroscience.** *Annu Rev Neurosci* 2009, **32**:435–506.
  3. Peterka DS, Takahashi H, Yuste R: **Imaging voltage in neurons.** *Neuron* 2011, **69**:9–21.
  4. Knöpfel T: **Genetically encoded optical indicators for the analysis of neuronal circuits.** *Nat Rev Neurosci* 2012, **13**:687.
  5. Hill D, Keynes R: **Opacity changes in stimulated nerve.** *J Physiol* 1949, **108**:278–281.
  6. Cohen L, Keynes R: **Changes in light scattering associated with the action potential in crab nerves.** *J Physiol* 1971, **212**:259–275.
  7. Cohen L: **Changes in neuron structure during action potential propagation and synaptic transmission.** *Physiol Rev* 1973, **53**:373–418.
  8. Iwasa K, Tasaki I, Gibbons RC: **Swelling of nerve fibers associated with action potentials.** *Science* 1980, **210**:338–339.
  9. Salzberg B, Obaid A, Gainer H: **Large and rapid changes in light scattering accompany secretion by nerve terminals in the mammalian neurohypophysis.** *J Gen Physiol* 1985, **86**:395–411.
  10. Salzberg BM, Obaid A: **Optical studies of the secretory event at vertebrate nerve terminals.** *J Exp Biol* 1988, **139**:195–231.
  11. Stepnoski R, *et al.*: **Noninvasive detection of changes in membrane potential in cultured neurons by light scattering.** *Proc Natl Acad Sci USA* 1991, **88**:9382–9386.
  12. Popovic MA, Carnevale N, Rozsa B, Zecevic D: **Electrical behaviour of dendritic spines as revealed by voltage imaging.** *Nat Commun* 2015, **6**:8436.
  13. Kuhn B, Roome CJ: **Primer to voltage imaging with ANNINE dyes and two-photon microscopy.** *Front Cell Neurosci* 2019, **13**.
  14. Tsytsarev VL, Lun-De, Kong, Voon Kien, Liu Yu-Hang, Erzurumlu Reha S, Olivo Malini, Thakor Nitish V: **Recent progress in voltage-sensitive dye imaging for neuroscience.** *J Nanosci Nanotechnol* 2014, **14**:4733–4744.
  15. Bando Y, Sakamoto M, Kim S, Ayzenshtat I, Yuste R: **Comparative evaluation of genetically encoded voltage indicators.** *Cell Rep* 2019, **26**:802–813. e804.
  16. Lin MZ, Schnitzer MJ: **Genetically encoded indicators of neuronal activity.** *Nat Neurosci* 2016, **19**:1142.
  17. Xu Y, Zou P, Cohen AE: **Voltage imaging with genetically encoded indicators.** *Curr Opin Chem Biol* 2017, **39**:1–10.
  18. Hochbaum DR, *et al.*: **All-optical electrophysiology in mammalian neurons using engineered microbial rhodopsins.** *Nat Methods* 2014, **11**:825.
  19. St-Pierre F, *et al.*: **High-fidelity optical reporting of neuronal electrical activity with an ultrafast fluorescent voltage sensor.** *Nat Neurosci* 2014, **17**:884.
  20. Gong Y, *et al.*: **High-speed recording of neural spikes in awake mice and flies with a fluorescent voltage sensor.** *Science* 2015, **350**:1361–1366.
  21. Piatkevich KD, *et al.*: **A robotic multidimensional directed evolution approach applied to fluorescent voltage reporters.** *Nat Chem Biol* 2018, **14**:352.
  22. Baker M: **Laser tricks without labels.** *Nat Methods* 2010, **7**:261–266.
  23. Boas DA, Dunn AK: **Laser speckle contrast imaging in biomedical optics.** *J Biomed Opt* 2010, **15**, 011109.
  24. Morone KA, Neimat JS, Roe AW, Friedman RM: **Review of functional and clinical relevance of intrinsic signal optical**

- imaging in human brain mapping. *NeuroPhotonics* 2017, **4**, 031220.
25. Iwasa K, Tasaki I: **Mechanical changes in squid giant axons associated with production of action potentials.** *Biochem Biophys Res Commun* 1980, **95**:1328–1331.
  26. Tasaki I, Iwasa K: **Rapid pressure changes and surface displacements in the squid giant axon associated with production of action potentials.** *Jpn J Physiol* 1982, **32**:69–81.
  27. Tasaki I, Byrne PM: **Large mechanical changes in the bullfrog olfactory bulb evoked by afferent fiber stimulation.** *Brain Res* 1988, **475**:173–176.
  28. Tasaki I, Byrne P: **Volume expansion of nonmyelinated nerve fibers during impulse conduction.** *Biophys J* 1990, **57**:633.
  29. Kim G, Kosterin P, Obaid A, Salzberg B: **A mechanical spike accompanies the action potential in mammalian nerve terminals.** *Biophys J* 2007, **92**:3122–3129.
  30. El Hady A, Machta BB: **Mechanical surface waves accompany action potential propagation.** *Nat Commun* 2015, **6**:6697.
  31. Gonzalez-Perez A, et al.: **Solitary electromechanical pulses in lobster neurons.** *Biophys Chem* 2016, **216**:51–59.
  32. Engelbrecht J, Peets T, Tamm K: **Electromechanical coupling of waves in nerve fibres.** *Biomechanics Model Mechanobiol* 2018, **17**:1771–1783.
  33. Yang Y, et al.: **Imaging action potential in single mammalian neurons by tracking the accompanying sub-nanometer mechanical motion.** *ACS Nano* 2018, **12**:4186–4193.
- The authors demonstrated optical imaging of morphological changes during action potential in single mammalian neurons using an edge tracking method. A spatial distribution map of membrane displacement is generated. The maximum displacement 0.3 nm on average.
34. Dipierro S, Valdinoci E: **A simple mathematical model inspired by the Purkinje cells: from delayed travelling waves to fractional diffusion.** *Bull Math Biol* 2018, **80**:1849–1870.
  35. Cohen L, Keynes R, Hille B: **Light scattering and birefringence changes during nerve activity.** *Nature* 1968, **218**:438.
  36. Graf BW, Ralston TS, Ko H-J, Boppart SA: **Detecting intrinsic scattering changes correlated to neuron action potentials using optical coherence imaging.** *Opt Express* 2009, **17**:13447–13457.
  37. Badreddine AH, Jordan T, Bigio IJ: **Real-time imaging of action potentials in nerves using changes in birefringence.** *Biomed Opt Express* 2016, **7**:1966–1973.
  38. LaPorta A, Kleinfeld D: **Interferometric detection of action potentials.** *Cold Spring Harb Protoc* 2012, **2012**, ip068148.
  39. Ling T, et al.: **Full-field interferometric imaging of propagating action potentials.** *Light Sci Appl* 2018, **7**:107.
- The authors used full-field interferometry and detected optical phase shift during spiking activity of HEK-293 cells. The phase shift signal correlates with the electrical signal recorded simultaneously.
40. Batabyal S, et al.: **Label-free optical detection of action potential in mammalian neurons.** *Biomed Opt Express* 2017, **8**:3700–3713.
  41. Fischer MC, et al.: **Self-phase modulation signatures of neuronal activity.** *Opt Lett* 2008, **33**:219–221.
  42. Macias-Romero C, et al.: **High throughput second harmonic imaging for label-free biological applications.** *Opt Express* 2014, **22**:31102–31112.
  43. Nemet BA, Nikolenko V, Yuste R: **Second harmonic imaging of membrane potential of neurons with retinal.** *J Biomed Opt* 2004, **9**:873–882.
  44. Araya R, Jiang J, Eishenthal KB, Yuste R: **The spine neck filters membrane potentials.** *Proc Natl Acad Sci USA* 2006, **103**:17961–17966.
  45. Nuriya M, Jiang J, Nemet B, Eishenthal KB, Yuste R: **Imaging membrane potential in dendritic spines.** *Proc Natl Acad Sci USA* 2006, **103**:786–790.
  46. Sacconi L, et al.: **Optical recording of electrical activity in intact neuronal networks with random access second-harmonic generation microscopy.** *Opt Express* 2008, **16**:14910–14921.
  47. Didier M, Tarun O, Jourdain P, Magistretti P, Roke S: **Membrane water for probing neuronal membrane potentials and ionic fluxes at the single cell level.** *Nat Commun* 2018, **9**:5287.
- The authors demonstrated label-free second harmonic imaging of neuronal membrane potential. The orientation of membrane interfacial water induced by the ion was used as a contrast to image changes in the membrane potential and K<sup>+</sup> ion flux.
48. Macias-Romero C, Nahalka I, Okur HI, Roke S: **Optical imaging of surface chemistry and dynamics in confinement.** *Science* 2017, **357**:784–788.
  49. Ong S, Zhao X, Eishenthal KB: **Polarization of water molecules at a charged interface: second harmonic studies of the silica/water interface.** *Chem Phys Lett* 1992, **191**:327–335.
  50. Gibbs-Davis JM, Kruk JJ, Konek CT, Scheidt KA, Geiger FM: **Jammed Acid–base reactions at interfaces.** *J Am Chem Soc* 2008, **130**:15444–15447.
  51. Tarun OB, Hanneschläger C, Pohl P, Roke S: **Label-free and charge-sensitive dynamic imaging of lipid membrane hydration on millisecond time scales.** *Proc Natl Acad Sci USA* 2018, **115**:4081–4086.
- The authors imaged membrane-bound water orientation on millisecond time scales by wide-field SHG microscopy. Using nonlinear optical theory, the electrostatic membrane potential map was constructed, indicating spatiotemporal fluctuation in the model membrane.
52. Verma SP, Wallach D: **Erythrocyte membranes undergo cooperative, pH-sensitive state transitions in the physiological temperature range: evidence from Raman spectroscopy.** *Proc Natl Acad Sci USA* 1976, **73**:3558–3561.
  53. Mikkelsen RB, Verma SP, Wallach D: **Effect of transmembrane ion gradients on Raman spectra of sealed, hemoglobin-free erythrocyte membrane vesicles.** *Proc Natl Acad Sci USA* 1978, **75**:5478–5482.
  54. Davis JG, Gierszal KP, Wang P, Ben-Amotz D: **Water structural transformation at molecular hydrophobic interfaces.** *Nature* 2012, **491**:582.
  55. Cheng J-X, Xie XS: *Coherent Raman scattering microscopy.* CRC Press; 2012.
  56. Min W, Freudiger CW, Lu S, Xie XS: **Coherent nonlinear optical imaging: beyond fluorescence microscopy.** *Annu Rev Phys Chem* 2011, **62**:507–530.
  57. Cheng J-X, Xie XS: **Vibrational spectroscopic imaging of living systems: an emerging platform for biology and medicine.** *Science* 2015, **350**, aaa8870.
  58. Yue S, Cárdenas-Mora JM, Chaboub LS, Lelièvre SA, Cheng J-X: **Label-free analysis of breast tissue polarity by Raman imaging of lipid phase.** *Biophys J* 2012, **102**:1215–1223.
  59. Shen Y, et al.: **Metabolic activity induces membrane phase separation in endoplasmic reticulum.** *Proc Natl Acad Sci USA* 2017, **114**:13394–13399.
  60. Liu B, et al.: **Label-free spectroscopic detection of membrane potential using stimulated Raman scattering.** *Appl Phys Lett* 2015, **106**:173704.
  61. Lee HJ, et al.: **Label-free vibrational spectroscopic imaging of neuronal membrane potential.** *J Phys Chem Lett* 2017, **8**:1932–1936.
- The authors identified spectroscopic signature of neuronal membrane potentials. Using high-speed stimulated Raman scattering imaging, mapping of subcellular distribution of membrane potential in a single mammalian neuron and multineuron voltage imaging in brain slices were demonstrated. This study also achieved single-trial action potential imaging in a single mammalian neuron using the spectroscopic signature identified.
62. Ji M, et al.: **Rapid, label-free detection of brain tumors with stimulated Raman scattering microscopy.** *Sci Transl Med* 2013, **5**. 201-119.

63. Evans CL, *et al.*: **Chemically-selective imaging of brain structures with CARS microscopy.** *Opt Express* 2007, **15**: 12076–12087.
64. Fu Y, Huff TB, Wang HW, Wang H, Cheng JX: **Ex vivo and in vivo imaging of myelin fibers in mouse brain by coherent anti-Stokes Raman scattering microscopy.** *Opt Express* 2008, **16**:19396–19409.
65. Fu Y, Wang H, Shi R, Cheng J-X: **Second harmonic and sum frequency generation imaging of fibrous astroglial filaments in ex vivo spinal tissues.** *Biophys J* 2007, **92**:3251–3259.
66. Raghunathan V, Han Y, Korth O, Ge N-H, Potma EO: **Rapid vibrational imaging with sum frequency generation microscopy.** *Opt Lett* 2011, **36**:3891–3893.
67. Witte S, *et al.*: **Label-free live brain imaging and targeted patching with third-harmonic generation microscopy.** *Proc Natl Acad Sci USA* 2011, **108**:5970–5975.
68. Jiang X, *et al.*: **Resolving voltage-dependent structural changes of a membrane photoreceptor by surface-enhanced IR difference spectroscopy.** *Proc Natl Acad Sci USA* 2008, **105**: 12113–12117.
69. Zhang D, *et al.*: **Depth-resolved mid-infrared photothermal imaging of living cells and organisms with submicrometer spatial resolution.** *Sci Adv* 2016, **2**, e1600521.
70. Bai Y, Zhang D, Li C, Liu C, Cheng J-X: **Bond-selective imaging of cells by mid-infrared photothermal microscopy in high wavenumber region.** *J Phys Chem B* 2017, **121**:10249–10255.
71. Li Z, Aleshire K, Kuno M, Hartland GV: **Super-resolution far-field infrared imaging by photothermal heterodyne imaging.** *J Phys Chem B* 2017, **121**:8838–8846.
72. Bai Y, *et al.*: **Ultrafast chemical imaging by widefield photothermal sensing of infrared absorption.** *Sci Adv* 2019, **5**, eaav7127.